Quasi Fermi level splitting of Cu-rich and Cu-poor Cu(In,Ga)Se2 absorber layers

Finn Babbe, Leo Choubrac, and Susanne Siebentritt

Articles you may be interested in

Structural and compositional analyses of Cu(In,Ga)Se2 thin film solar cells with different cell performances
J. Vac. Sci. Technol. B **34**, 03H121 (2016); 10.1116/1.4943518

Diffusion barrier properties of molybdenum back contacts for Cu(In,Ga)Se2 solar cells on stainless steel foils
J. Appl. Phys. **113**, 054506 (2013); 10.1063/1.4789616

Electronic effect of Na on Cu(In,Ga)Se2 solar cells
Appl. Phys. Lett. **101**, 023901 (2012); 10.1063/1.4733679

Atom probe study of Cu-poor to Cu-rich transition during Cu(In,Ga)Se2 growth
Appl. Phys. Lett. **99**, 232108 (2011); 10.1063/1.3665948

Diffusions in (In,Se)– Cu(In,Ga)Se 2 / SnO 2 thin film structures
J. Appl. Phys. **88**, 5710 (2000); 10.1063/1.1320005

Quasi Fermi level splitting of Cu-rich and Cu-poor Cu(In,Ga)Se$_2$ absorber layers

Finn Babbe,[a)] Leo Choubrac, and Susanne Siebentritt

Laboratory for Photovoltaics, Physics and Material Science Research Unit, University of Luxembourg, 41, Rue de Brill, L-4422 Belvaux, Luxembourg

The quasi Fermi level splitting is measured for Cu(In,Ga)Se$_2$ absorber layers with different copper to (indium + gallium) ratios and for different gallium contents in the range of 20%–40%. For absorbers with a [Cu]/[In + Ga] ratio below one, the measured quasi Fermi level splitting is 120 meV higher compared to absorbers grown under copper excess independent of the gallium content, contrary to the ternary CuInSe$_2$ where the splitting is slightly higher for absorber layers grown under copper excess. Possible explanations are the gallium gradient determined by the secondary ion mass spectrometry measurement which is less pronounced towards the surface for stoichiometric absorber layers or a fundamentally different recombination mechanism in the presence of gallium. Comparing the quasi Fermi level splitting of an absorber to the open circuit voltage of the corresponding solar cell, the difference for copper poor cells is much lower (60 meV) than that for copper rich cells (140 meV). The higher loss in V$_{OC}$ in the case of the Cu-rich material is attributed to tunneling enhanced recombination due to higher band bending within the space charge region. *Published by AIP Publishing.* [http://dx.doi.org/10.1063/1.4961530]

Chalcopyrite solar cells with copper indium gallium di-selenide Cu(In,Ga)Se$_2$ (CIGS) absorber layers have the highest efficiencies of all thin film photovoltaic materials, reaching 22.6%[1] cell efficiency on the laboratory scale and up to 17.9%[2] industrial module efficiency. All records and in fact all commercial modules as well as most of the laboratory cells use non stoichiometric absorbers with [Cu]/([Ga] + [In]) (CGI) well below 1.

In this publication, absorber layers with CGI below 1 are denoted as Cu-poor and absorber layers with CGI above 1 are denoted as Cu-rich. Absorbers grown with a CGI above 1 form stoichiometric CIGS and a secondary phase of copper selenide. After etching with potassium cyanide (KCN), the secondary phases are removed and all Cu-rich absorbers are stoichiometric. The stability of the ternary semiconductor in the Cu-poor part of the phase diagram is possible due to the introduction of defects into the crystal structure, leading to lower carrier lifetimes and inferior transport properties.[3] CIGS layers grown under copper excess have a lower defect density but solar cells are dominated by recombination near the interface with a CdS buffer layer and thus show a strong decrease in the open circuit voltage (V$_{oc}$).[3,4] With absolute calibrated photoluminescence (PL) experiments on etched absorber layers at room temperature, it is possible to measure the quasi Fermi level splitting (qFLs) μ which is an upper limit for the open circuit voltage.[5–8] A material with a high recombination rate will show a low qFLs due to a lower density of photo-generated charge carriers. Thus, the qFLs gives a direct assessment of the quality of the absorber layer without the need of finishing the solar cell. For pure copper indium di-selenide CuInSe$_2$ (CIS) without gallium, the qFLs in Cu-poor films is lower than for Cu-rich films, albeit only by 50 meV.[3,9,10] However, in finished solar cells, the Cu-rich

material shows a 90 mV lower V$_{oc}$ than its non-stoichiometric counterpart. The degradation of the qFLs of bare absorbers exposed to air shows an exponential decay behavior[9] for both materials. The decay is entirely driven by the formation of In$_2$O$_3$[11] at the surface causing enhanced recombination and reduced minority carrier life time.[9] Absorbers with overall copper poor composition show a more prominent decrease of the qFLs with a decay constant of approximately 30 min in comparison to polycrystalline Cu-rich absorbers with a decay constant of roughly 650 min. All absorbers can be refreshed to their as grown value by a KCN etch.[9] This paper investigates the behavior of the qFLs of Cu-rich and Cu-poor Cu(In,Ga)Se$_2$ films.

Polycrystalline CIGS samples have been prepared in a modified 3-stage-coevaporation process on molybdenum coated soda lime glass substrates in a molecular beam epitaxy system.[12,13] The CGI ratio is controlled by the length of the third stage. The overall elemental composition of grown absorbers is determined by energy dispersive x-ray spectroscopy (EDX). The investigated Cu-poor samples have a CGI of 0.9 while the Cu-rich samples have a CGI of roughly 1.2. After growth, a 5 min etching in 10% aqueous KCN solution removes the excess copper selenide from the surface of the Cu-rich samples. The Cu-poor samples are etched in 5% aqueous KCN solution for only 30 s to remove traces of oxides. The cells are finished with a 50 nm thick CdS buffer layer applied by chemical bath deposition, a sputtered double layer of undoped and aluminium doped zinc oxide and nickel/aluminum grids. Six samples with Cu-poor composition and [Ga]/([Ga] + [In]) (GGI) ratios between 0.25 and 0.38 are compared to eight samples with overall Cu-rich composition after growth with GGI values ranging from 0.26 to 0.45.

For the photoluminescence (PL) experiments, a continuous wave argon ion laser with a wavelength of 514.5 nm is

a)Electronic mail: Finn.Babbe@uni.lu

used for optical excitation because of its long term power output stability. For photon counting and thus the determination of the qFLs, two corrections are applied to the raw data. The spectral correction is carried out using a commercial calibration lamp with a known spectrum. For the intensity correction, the beam diameter is measured with a CCD-camera and the laser power with a power meter. With this, the incident photon flux is calculated and tuned to be twice the photon flux of the AM 1.5 sun spectrum above the bandgap. The calibrated luminescence spectra are converted to energy space and evaluated by means of Planck's generalized law[5] which describes the PL-yield depending on the energy as a function of absorptivity, temperature, and the qFLs. By fitting the high energy slope at photon energies sufficiently larger than the bandgap, the absorptivity can be assumed unity and thus the qFLs extracted[7,10] (additional details are in the supplementary material). Before each PL measurement series was performed, the prepared absorber layers are etched in the same way as for cell preparation and directly transferred to the calibrated PL set up. The time between etching and the first PL measurement is approximately 3 min.

The current voltage characteristics (IV) of finished cells are measured under 100 mW/cm^2 illumination of a halogen cold mirror lamp. Furthermore, the external quantum efficiency (EQE) was determined and the electronic band gap (E_g) extracted from a linear extrapolation.

To confirm the lower defect concentration of Cu-rich absorber layers, illumination dependent PL measurements are carried out at a temperature of 10 K. For Cu-poor materials, one broad PL-peak caused by the compensation of the material is expected[14,15] whereas for a Cu-rich material with good crystal structure, a few narrow peaks should be detectable.[16] All Cu-poor samples show, as expected, one broad asymmetric peak, which is exemplary plotted in Fig. 1 in black and shifted upwards for better clarity. By plotting the integrated area below the curve half logarithmically over the excitation power, a k-value, according to Ref. 17, of (0.97 ± 0.01) can be determined as an average over all Cu-poor samples. Furthermore, a peak shift of (10 ± 1) meV per decade is extracted. Those values fit literature data for a
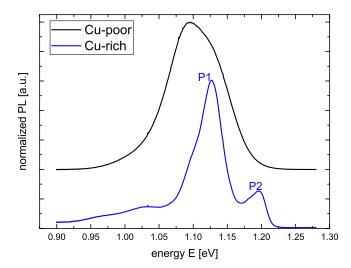
strongly compensated donor acceptor transition very well, for which a shift of about 10 meV per decade and a k value equal or below 1 are expected. For all Cu-rich samples, at least two peaks per sample could be measured. Those peaks are much narrower compared to the Cu-poor counterparts, shown in blue at the bottom of Fig. 1. The peak centered at lower energies (P1) shows a peak shift with excitation of a few meV per decade and the peak centered at higher energies (P2) shows a shift below 0.5 meV per decade. The exemplary sample shows a k value of 0.86 for P1 and a k value of 1.6 for P2. Those values indicate at least one donor-acceptor transition (P1) and an excitonic transition (P2). Temperature dependent measurements show an activation energy of 5 meV for P1 further suggesting a bound excitonic transition. This confirms the thesis of a better crystal structure of the Cu-rich samples compared to Cu-poor samples investigated within this study.

In Fig. 2, a time dependent qFLs μ measurement is depicted for one Cu-poor with a bandgap of 1.17 eV and one Cu-rich absorber with a bandgap of 1.14 eV, which both have a GGI of roughly 0.3. The measured values decrease over time for both materials with similar decay times due to oxidation of the surface. The qFLs values for stoichiometric absorbers are well below the ones for Cu-poor absorbers in contrast to the observation in CIS.[9] The description of the decay behavior with an exponential function, according to Regesch *et al.*[9] as shown in the graph, does not describe the data accurately. Especially when plotted semi-logarithmically against time, the data show more than one linear region, indicating that the oxidation of the surface is more involved in the case of CIGS than in the case of CIS. The results of the evaluation with this method are strongly dependent on the fitted region and vary even between similar samples. Thus, the results of the fit are not reliable and will not be used to categorize the samples. In general, the extracted decay constant τ is in the range of 20 min for Cu-poor samples and about 35 min for Cu-rich samples. The strong difference between decay constants in Cu-rich and
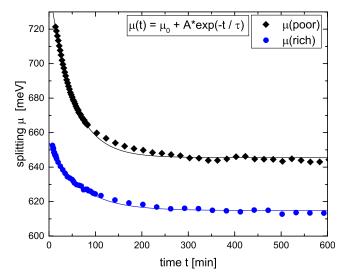

FIG. 1. Measured photoluminescence spectra of a Cu-poor (top, shifted upwards for better visibility) and a Cu-rich (bottom) Cu(In,Ga)Se$_2$ absorber at 10 K.

FIG. 2. QFLs μ of a Cu-poor (black diamonds) and a Cu-rich (blue circles) Cu(In,Ga)Se$_2$ absorber after etching as a function of time. Solid lines are exponential fits with the displayed equation according to the work of Regesch *et al.*[9]

Cu-poor CIS absorbers of 650 min to 30 min (Ref. 9) cannot be verified for CIGS.

Since the fitting is not adequate and we cannot use it to extrapolate the qFLs directly after etching, the very first data point of each time series is used to compare the qFLs between different samples. In Fig. 3, the obtained values are plotted against the electronic band gap determined from EQE, which corresponds to the bandgap of the minimum of the gallium gradient.[18] All Cu-poor samples show a higher qFLs regardless of the bandgap/the amount of gallium. The solid lines depict a linear fit to the data with a fixed slope of 1, assuming a linear relationship between splitting and bandgap. This may not hold true for the whole bandgap range from 1 eV for CIS to 1.7 eV for copper gallium di-selenide CuGaSe$_2$ (CGS) but is sufficient for the limited energy range investigated.

The fitting shows a (120 ± 10) meV lower qFLs for the Cu-rich samples which is inconsistent compared to the results for CIS[9] where Cu-rich has a slight advantage in the case of the bare absorber. A possible explanation for this difference could be the GGI gradient within the layer that can be expected in samples prepared by a 3-stage process. To verify this assumption, secondary ion mass spectrometry (SIMS) measurements were carried out. To scale the relative gallium and indium counts acquired, it is assumed that the bandgap from EQE corresponds to the bandgap of the minimum of the gallium gradient. In Fig. 4, the extracted GGI ratios from the SIMS measurement of the absorber are shown for one Cu-rich and for one Cu-poor with similar compositions. The corresponding bandgap was calculated assuming a bandgap bowing according to Alonso et al.[19] Since the overall copper composition was varied by changing the length of the third stage, the Cu-rich samples are a bit thinner.

Both curves show a strong gallium gradient towards the back contact, increasing the collection efficiency and reducing recombination at the molybdenum interface. The gallium gradient towards the front is much more pronounced for the Cu-poor samples but also measurable in the case of the
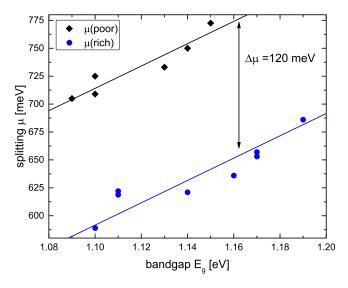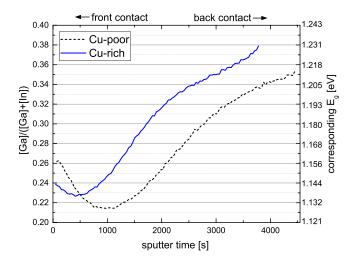

FIG. 4. GGI profiles determined from the SIMS measurement of a Cu-poor absorber (black) and a Cu-rich absorber (blue) plotted over the sputter time.

Cu-rich sample. This leads to a difference of the bandgap at the surface and the minimum of the gallium profile of about 10 meV in the case of Cu-rich and 40 meV for Cu-poor samples. The difference in qFLs can be explained by reduced surface recombination due to the more prominent gallium gradient towards the surface in case of Cu-poor absorbers or by a fundamental difference in the recombination mechanism between CIS and CIGS. For the latter one, we propose the Ga$_{Cu}$ antisite defect as a deep donor. In the case of a Cu-poor composition, this defect is predominantly in a complex form with two copper vacancies (Ga$_{Cu}$ + 2 V$_{Cu}$)[20] forming a donor type defect which is less deep inside the bandgap. In the case of a Cu-rich composition, the number of copper vacancies is greatly reduced leading to more gallium antisite defects which are not passivated and thus a decrease of the qFLs. An error of the measured PL spectra due to the gallium gradient can be excluded, since it is assumed that the PL is emitted from the bandgap minimum. This assumption is supported by measurements with different excitation wavelengths and thus different penetration depths that show identical spectra without any shift of the peak position. PL measurements from the backside measured on layers which were physically removed from the molybdenum back contact also show a peak at the same energy.

It has been shown that a thin layer of CdS applied by chemical bath deposition is sufficient to passivate the surface of CIS absorber layers for months.[9] The same effect has been observed for Cu(In,Ga)Se$_2$ samples investigated here. Comparing the very first measurements after the KCN etching of a bare absorber to the data of the same absorber with a passivation layer, no difference is observed. Averaging over all samples results in a deviation of $\Delta\mu = (-4 \pm 8)$ meV.

To compare the measured qFLs to the V$_{oc}$, we have to correct for the different illumination conditions during PL (2 suns) and IV (1 sun) measurements, since both values increase logarithmically with illumination. For this reason, the splitting of passivated absorbers was measured under various illumination conditions equivalent to a range from 0.5 to 20 suns. From the semi logarithmic plot of the qFLs over the illumination, the difference between 1 and 2 suns was

FIG. 3. QFLs of Cu-poor (black diamonds) and Cu-rich (blue circles) Cu(In,Ga)Se$_2$ absorber layers plotted against their electrical bandgap measured under illumination equivalent to two suns. The solid lines represent linear fits with a fixed slope of 1.

determined by a linear fit through all data points. Averaging over all samples, an offset of (26 ± 3) meV was derived. In Fig. 5, the corrected qFLs is plotted together with the V_{oc} of the finished cell against the bandgap. Since the qFLs is an upper limit for the V_{oc}, it is not surprising that the values for the V_{oc} are lower than that for the qFLs. In the case of the Cu-poor samples, 60 meV is lost when finishing the solar cell. For the Cu-rich samples, a loss of 140 meV is determined. The greater loss after finishing the solar cell in the case of Cu-rich samples has also been measured for pure CIS[9] and is attributed to stronger band bending within the space charge region which increases recombination close to the interface as well as tunneling enhanced recombination.[21] To verify this for the investigated samples, temperature dependent current voltage measurements were carried out and fitted with ECN's IVFit program.[22] The extrapolation of the V_{oc} above 200 K to 0 K yields the activation energy of the main recombination path.[23] For the Cu-poor sample, an activation energy close the bandgap is extracted indicating that the sample is limited by bulk recombination (graph S3 in the supplementary material). For the Cu-rich sample, the extracted value at 0 K is 280 meV below the bandgap which indicates that the sample is limited by interface recombination. From the IV fit also the diode ideality factor is extracted. For the Cu-rich sample, the ideality factor increases from 1.9 at room temperature to 3.6 at 200 K while it only increases slightly in the case of the Cu-poor sample (graph S4 in the supplementary material). This strong temperature dependence for samples grown under copper excess can be explained by tunneling enhanced recombination or multi step recombination.[23] These data suggest that the V_{oc} in Cu-rich CIGS is reduced by tunneling enhanced recombination, as already shown in CIS.

Low temperature PL measurements show a high crystal quality for Cu-rich materials for the whole range from CIS to CGS.[16] This property was verified within the used samples by PL measurements at 10 K. Previously, it was reported that the Cu-rich material shows higher qFLs values for the ternary CuInSe$_2$. Here, the influence of Cu-excess on the qFLs

for Cu(In,Ga)Se$_2$ was studied. It was shown that the qFLs of bare Cu-poor Cu(In,Ga)Se$_2$ absorber layers grown by a three-stage process is 120 meV higher than that of their Cu-rich counterparts, contrary to what has been observed for CuInSe$_2$. A possible explanation could be the reduced surface recombination due to a more prominent gallium gradient towards the front in the case of Cu-poor samples compared to Cu-rich samples shown by SIMS measurements or a fundamentally different recombination mechanism in the presence of gallium (e.g., Ga$_{Cu}$). The quasi Fermi level splitting after the deposition of cadmium sulfide is comparable with respect to the qFLs on the bare absorbers. When processed to solar cells, the V_{oc} decreases about 60 mV for Cu-poor absorbers and about 140 mV for Cu-rich ones. The higher loss in the case of the Cu-rich material is attributed to interface recombination and enhanced tunneling recombination due to higher band bending within the space charge region.

See supplementary material for detailed evaluation of the photoluminescence data in terms of quasi Fermi level splitting as well as for the temperature dependent current voltage analysis of finished solar cells.

[1]P. Jackson, R. Wuerz, D. Hariskos, E. Lotter, W. Witte, and M. Powalla, Phys. Status Solidi RRL **10**(8), 583 (2016).
[2]See http://www.avancis.de/presse/newsansicht/article/avancis-erzielt-erneuten-wirkungsgradrekord-fraunhofer-ise-zertifiziert-cigs-solarmodul-mit-wirkungsgrad-von-179/ for press release AVANCIS (last accessed May 2, 2016).
[3]S. Siebentritt, L. Gütay, D. Regesch, Y. Aida, and V. Depredurand, Sol. Energy Mater. Sol. Cells **119**, 18–25 (2013).
[4]M. Turcu, O. Pakma, and U. Rau, Appl. Phys. Lett. **80**, 2598–2600 (2002).
[5]P. Würfel, J. Phys. C: Solid State Phys. **15**(18), 3967 (1982).
[6]P. Würfel, *The Physics of Solar Cells* (Wiley-VCH, 2009).
[7]T. Unold and L. Gütay, "Photoluminescence Analysis of Thin-Film Solar Cells," in *Advanced Characterization Techniques for Thin Film Solar Cells*, edited by D. Abou-Ras, T. Kirchartz and U. Rau (Wiley-VCH, 2011), pp. 151–175.
[8]L. Gütay and G. H. Bauer, Thin Solid Films **517**(7), 2222–2225 (2009).
[9]D. Regesch, L. Gütay, J. K. Larsen, V. Depredurand, D. Tanaka, Y. Aida, and S. Siebentritt, Appl. Phys. Lett. **101**(11), 112108 (2012).
[10]L. Gütay, D. Regesch, J. K. Larsen, Y. Aida, V. Depredurand, and S. Siebentritt, Appl. Phys. Lett. **99**, 151912 (2011).
[11]A. Nelson, S. Gebhard, L. Kazmerski, E. Colavita, M. Engelhardt, and H. Höchst, Appl. Phys. Lett. **57**, 1428–1430 (1990).
[12]A. Gabor, J. Tuttle, D. Albin, M. Contreras, R. Noufi, and A. Herman, Appl. Phys. Lett. **65**, 198–200 (1994).
[13]L. Choubrac, T. Bertram, H. ElAnzeery, and S. Siebentritt, "Cu(In,Ga)Se$_2$ solar cells with improved current based on surface treated stoichiometric absorbers," Phys. Status Solidi (a) (submitted).
[14]A. Bauknecht, S. Siebentritt, J. Albert, and M. C. Lux-Steiner, J. Appl. Phys. **89**(8), 4391–4400 (2001).
[15]S. Siebentritt, N. Rega, A. Zajogin, and M. C. Lux-Steiner, Phys. Status Solidi C **1**(9), 2304–2310 (2004).
[16]N. Rega, S. Siebentritt, J. Albert, S. Nishiwaki, A. Zajogin, M. Ch. Lux-Steiner, R. Kniese, and M. J. Romero, Thin Solid Films **480–481**, 286–290 (2005).
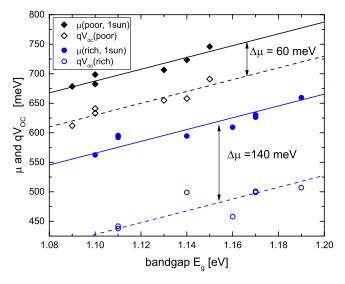

FIG. 5. QFLs of Cu-poor (closed diamonds) and Cu-rich (closed circles) Cu(In,Ga)Se$_2$ absorber layers as well as the corresponding V_{oc} (open symbols) for 1 sun illumination.

[17]S. Siebentritt and U. Rau, *Wide-Gap Chalcopyrites*, Springer Series in Material Science Vol. 86 (Springer, 2006).

[18]T. Dullweber, U. Rau, M. A. Contreras, R. Noufi, and H. Schock, IEEE Trans. Electron Devices **47**(12), 2249–2254 (2000).

[19]M. Alonso, M. Garriga, C. A. Durante Rincon, E. Hernandez, and M. Leon, Appl. Phys. A: Mater. Sci. Process. **74**(5), 659–664 (2002).

[20]B. Huang, S. Chen, H.-X. Deng, L.-W. Wang, M. A. Contreras, R. Noufi, and S.-H. Wei, IEEE J. Photovoltaics **4**(1), 477–482 (2014).

[21]V. Depredurand, T. Bertram, D. Regesch, B. Henx, and S. Siebentritt, Appl. Phys. Lett. **105**, 172104 (2014).

[22]A. Burgers, J. Eikelboom, A. Schönecker, and W. Sinke, in *Proceedings of the 25th IEEE PVSC Conference*, Washington DC (1996), pp. 569–572.

[23]T. Kirchartz, K. Ding, and U. Rau, "Fundamental Electrical Characterization of Thin-Film Solar Cells," in *Advanced Characterization Techniques for Thin Film Solar Cells*, edited by D. Abou-Ras, T. Kirchartz and U. Rau (Wiley-VCH, 2011), pp. 35–60.